3,3′-Diindolylmethane Inhibits Prostate Cancer Development in the Transgenic Adenocarcinoma Mouse Prostate Model

Han Jin Cho,[1] So Young Park,[1] Eun Ji Kim,[3] Jin-Kyung Kim,[3] and Jung Han Yoon Park[1,2,3]*

[1]*Department of Food Science and Nutrition, Hallym University, Chuncheon, Korea*
[2]*Medical & Bio-Materials Research Center, Hallym University, Chuncheon, Korea*
[3]*Center for Efficacy Assessment and Development of Functional Foods and Drugs, Hallym University, Chuncheon, Korea*

3,3′-Diindolylmethane (DIM) is a major in vivo derivative of indole-3-carbinol, which is present in cruciferous vegetables and has been reported to possess anti-carcinogenic properties. In the present study, we examined whether DIM inhibits the development of prostate cancer using the transgenic adenocarcinoma mouse prostate (TRAMP) model. DIM feeding inhibited prostate carcinogenesis in TRAMP mice, reduced the number of cells expressing the SV40 large tumor antigen and proliferating cell nuclear antigen, and increased the number of terminal dUTP nick-end labeling-positive cells in the dorsolateral lobes of the prostate. Additionally, DIM feeding reduced the expression of cyclin A, cyclin-dependent kinase (CDK)2, CDK4, and Bcl-xL, and increased p27 and Bax expression. To assess the mechanisms by which DIM induces apoptosis, LNCaP and DU145 human prostate cancer cells were cultured with various concentrations of DIM. DIM induced a substantial reduction in the numbers of viable cells and induced apoptosis in LNCaP and DU145 cells. DIM increased the cleavage of caspase-9, -7, -3, and poly (ADP-ribose) polymerase (PARP). DIM increased mitochondrial membrane permeability and the translocation of cytochrome c and Smac/Diablo from the mitochondria. Additionally, DIM induced increases in the levels of cleaved caspase-8, truncated Bid, Fas, and Fas ligand, and the caspase-8 inhibitor Z-IETD-FMK was shown to mitigate DIM-induced apoptosis and the cleavage of caspase-3, PARP, and Bid. These results indicate that DIM inhibits prostate carcinogenesis via induction of apoptosis and inhibition of cell cycle progression. DIM induces apoptosis in prostate cancer cells via the mitochondria- and death receptor-mediated pathways.

Key words: DIM; prostate cancer; TRAMP; caspase; apoptosis; Fas

INTRODUCTION

Prostate cancer is the most frequently diagnosed cancer among men in the United States [1]. Although the exact causes of prostate cancer are currently unknown, several risk factors have been associated with prostate cancer, including age, race, family history, and diet [2,3]. As the incidence of this disease increases with age and prostate cancer is a relatively slow-growing variety of cancer, chemoprevention utilizing dietary agents is considered to be an effective means for slowing the development of prostate cancer.

Previous epidemiological studies have demonstrated that diets rich in cruciferous vegetables, such as broccoli, Brussel sprouts, cabbage, and cauliflower are associated with lowered risk of prostate cancer development [4–6]. Indole-3-carbinol (I3C), a major bioactive component present in these vegetables [7], has been shown to exert chemopreventive effects in prostate cancer [8]. However, in the low-pH environment of the stomach, I3C is converted rapidly into many self-condensation products; 3,3′-diindolylmethane (DIM) being the principal product [9], thus suggesting that DIM may mediate the biological effects of I3C. DIM has been reported to induce G1 arrest in human prostate cancer cells in culture via an induced reduction in the expression of cyclin-dependent kinase (CDK)2 and CDK4 proteins and an increase in $p2^{KIP1}$ expression [10]. Additionally, DIM has been previously reported to induce apoptosis and increase the release of cytochrome c from mitochondria in human prostate cancer cells [11,12]. However, the molecular mechanisms underlying the DIM-mediated apoptosis of prostate cancer cells have yet to be studied in detail.

Abbreviations: I3C, indole-3-carbinol; DIM, 3,3′-diindolylmethane; CDK, cyclin-dependent kinase; TRAMP, transgenic adenocarcinoma mouse prostate; T-ag, tumor antigen; PARP, poly (ADP-ribose) polymerase; PCNA, proliferating cell nuclear antigen; GU, genitourinary; WDC, well-differentiated carcinoma; TUNEL, terminal dUTP nick-end labeling.

Han Jin Cho and So Young Park contributed equally to this work.

Disclosure statement: No potential conflicts of interest are disclosed.

*Correspondence to: Department of Food Science and Nutrition, Hallym University, 39 Hallymdaehak-gil, Chuncheon 200-702, Korea.

Received 29 May 2009; Revised 30 September 2010; Accepted 1 October 2010

DOI 10.1002/mc.20698

Published online 8 November 2010 in Wiley Online Library (wileyonlinelibrary.com).

Because a common feature of cancer cells is their ability to evade apoptosis, the induction of apoptosis in malignant cells is one of the most effective strategies for the prevention and/or treatment of cancer. In addition to synthetic drugs, researchers are increasingly searching for bioactive food components with the ability to regulate apoptotic signaling pathways because of their low toxicity. The apoptosis induced by a variety of caspases is initiated by two separate signals—one extrinsic and the other intrinsic. The extrinsic apoptotic pathway is activated through death receptors, which themselves are activated by specific death ligands, such as TRAIL and Fas-ligand, thereby inducing caspase activation [13]. In the intrinsic apoptotic pathway, the Bcl-2 family proteins perform a pivotal function in the regulation of the permeability of mitochondrial membranes. Anti-apoptotic Bcl-2 family proteins such as Bcl-2 and Bcl-xL reduce membrane permeability, whereas pro-apoptotic Bcl-2 proteins including Bax, Bid, and Bad increase membrane permeability. The increase in membrane permeability results in the release of cytochrome c into the cytoplasm, which induces the formation of apoptosomes that harbor a number of Apaf-1 molecules that recruit and activate caspase-9 [14].

In vivo animal studies have previously demonstrated that DIM inhibits the growth of prostate tumor resulting from the subcutaneous injection of TRAMP-C2, a mouse prostate cancer cell line [15]. Subcutaneous sites are not orthotopic and do not represent appropriate sites for human tumors [16]. Although these subcutaneous xenograft models have been previously utilized as preclinical models for anticancer drug activity, they may not ultimately prove to be appropriate animal models for the assessment of the effects of agents on the development and progression of human prostate cancer. Transgenic adenocarcinoma mouse prostate (TRAMP) mice were developed by Greenberg using the prostate-specific rat probasin promoter (−426/+28) to drive the expression of the SV40 large tumor antigen (T-ag)-coding region specifically in the prostatic epithelium [17]. The T-ag abrogates the function of retinoblastoma (Rb) and p53, and thus operates as an oncoprotein. It has been reported that cancer develops spontaneously in the original tissue microenvironment and progresses through multiple stages, as does human prostate cancer; this is the principal advantage of this transgenic model. This model was generally considered to closely mimic the histological progression of human prostate cancer [17,18].

The primary objective of the present study, then, was to determine whether DIM suppresses prostate cancer development in TRAMP mice. We also attempted to identify the mechanisms by which DIM induces the apoptosis of prostate cancer cells using the human prostate cancer cell lines, LNCaP (androgen receptor positive, wild-type p53) and DU145 (androgen receptor-negative, mutated p53 and Rb) cells [19–21].

MATERIALS AND METHODS

Materials and Reagents

The following reagents were purchased: DIM (LKT Laboratories, Inc., St. Paul, MN); horse-radish peroxidase (HRP)-conjugated anti-rabbit and anti-mouse IgG from Amersham (Arlington Heights, IL); 3-[4,5-dimethylthiazol-2-yl]-2,5-diphenyltetrazolium bromide (MTT) and anti-β-actin from Sigma (St. Louis, MO); antibodies against cleaved caspase-3, cleaved caspase-7, cleaved caspase-9, cleaved caspase-8, cleaved poly (ADP-ribose) polymerase (PARP), Bid, and Bcl-xL from Cell Signaling (Beverly, MA); antibodies against CDK2, CDK4, cyclin A, p27, Smac/Diablo, Bcl-2, Bax, Fas, Fas-L, proliferating cell nuclear antigen (PCNA), and heat shock protein 60 (HSP60) from Santa Cruz Biotechnology (Santa Cruz, CA); and cytochrome c antibody, phycoerythrin (PE)-conjugated annexin V (annexin V-PE) and 7-amino-actinomycin D (7-AAD), and anti-T-ag antibody from BD Pharmingen (Franklin Lake, NJ).

Animals and Treatments

All animal experiments were approved by the Animal Care and Use Committee of Hallym University (Chuncheon, Korea) and conducted in accordance with the University's Guidelines for the Care and Use of Laboratory Animals. Heterozygous TRAMP females and nontransgenic C57BL/6 breeder males were purchased from the Jackson Laboratory (Bar Harbor, ME) and maintained under specific pathogen-free (SPF) conditions on a commercial unpurified rodent diet (containing 234 g/kg protein, 100 g/kg fat, 5.3 g/kg crude fiber, and 69 g/kg ash; Superfeed Co., Wonju, Korea) and water ad libitum. Mouse tail DNA was isolated with an Extract-N-Amp™ Tissue PCR kit (Sigma) and the TRAMP animals were genotyped via PCR-based DNA screening, as described previously [22]. Male TRAMP mice and their nontransgenic littermates at 6 wk of age were randomly divided into control and DIM-treatment groups and gavage-fed with 0 (vehicle), 10, or 20 mg/kg of DIM every other day (TRAMP, 8 mice/group; normal, 6 mice/group). DIM was dissolved in DMSO and diluted with corn oil at a ratio of 1:99 (v/v). All mice were sacrificed at 22 wk of age, and the genitourinary (GU) tract was removed, weighed, and fixed in 4% paraformaldehyde.

Immunohistochemical Analysis

The paraffin-embedded sections (5 μm) were stained with Hematoxylin and Eosin (H&E). Each pathologic grade [prostatic intraepithelial neoplasia (PIN) and well-differentiated carcinoma (WDC)] in the dorsolateral lobes of the prostate (DP) was scored

in accordance with the histologic grading system described for TRAMP [23].

For immunohistochemistry, endogenous peroxidases were quenched for 10 min with 3% hydrogen peroxide. The sections were then incubated with their relevant antibodies at 1:250 dilutions overnight at 4°C. The following steps were continued using an LSAB^{+} kit (Dako, Carpinteria, CA) in accordance with the manufacturer's instructions. Sections were counterstained with hematoxylin, dehydrated through a graded series of alcohol into xylene, and mounted under glass coverslips. Apoptotic cells were identified via terminal dUTP nick-end labeling (TUNEL) staining using a DeadEnd^{TM} Fluorometric TUNEL System (Promega, Madison, WI).

Cell Culture

DU145 and LNCaP cells were obtained from the American Type Culture Collection (Manassas, VA) and maintained in DMEM/F12 containing 10% FBS with 100 000 U/L of penicillin and 100 mg/L of streptomycin. In order to evaluate the effects of DIM, we plated the cells on multi-well plates with DMEM/F-12 containing 10% FBS. Before administering DIM treatment, the cell monolayers were rinsed and serum-deprived for 24 h with DMEM/F-12 supplemented with 1% (DU145) or 5% (LNCaP) charcoal stripped FBS (serum-deprivation medium, SDM). After serum deprivation, cells were incubated in SDM containing the various concentrations (0–30 μmol/L) of DIM. Viable cell numbers were estimated by the MTT assay.

In order to detect time-dependent apoptotic cell death, the cells were treated with 30 μmol/L of DIM for 12, 24, or 48 h. The cell lysates were then assayed for quantitative determinations of mono- and oligonucleosomes released into the cytoplasm using a Cell Death Detection ELISA^{PLUS} kit (Roche Applied Science, Mannheim, Germany), based on the manufacturer's recommendations.

Fluorescence-Activated Cell Sorting (FACS) Analysis

In order to quantify the numbers of apoptotic cells, cells were plated in 24-well plates and treated with various concentrations of DIM as described above. In order to inhibit caspase-8 activity, the cells were pretreated for 4 h with 20 μmol/L of Z-IETD-FMK (R & D System, Minneapolis, MN) before treatment with 30 μmol/L of DIM. The cells were trypsinized and incubated with annexin V-PE and 7-AAD for 15 min at room temperature in darkness. Living cells and early apoptotic cells were analyzed via flow cytometry within 1 h using a FACScan^{TM} system (Becton Dickinson, Franklin Lake, NJ).

In order to quantify the number of cells with depolarized mitochondrial membranes, the DIM-treated cells were stained with JC-1 (Sigma) and analyzed via flow cytometry with a FACScan^{TM} system, as described previously [24].

Western Blot Analysis

Total cell lysates were prepared as previously described [25] and the mitochondrial and cytosolic proteins were separated as described by Eguchi et al. [26]. The total cell lysates, mitochondrial fractions, and cytosolic fractions were utilized for Western blot analysis with their relevant antibodies, as described previously [24]. The abundance of each band was quantified using the Bio-profile Bio-1D application (Vilber-Lourmat, Marine La Vallee, France), and the expression levels were normalized to β-actin. The purity of the mitochondrial and cytosolic preparations were estimated via Western blotting with an antibody raised against mitochondrial HSP60 [27] and COX-1 [28].

Caspase-3 Activity Assay

A Caspase-3 Colorimetric Assay Kit (Biovision, Mountain View, CA) was used to detremine caspase-3 activity, in accordance with the manufacturer's recommendations. In brief, the cells were treated for 48 h with 0–30 μmol/L of DIM. The cell lysates (100 μg of protein) were mixed with the reaction buffer and 200 μmol/L of DEVE-*p*NA substrate and incubated for 4 h at 37°C. The absorbance was subsequently measured at 405 nm.

Statistical Analysis

The results were expressed as means ± SEM, and analyzed via analysis of variance. Differences among the treatment groups were assessed by Duncan's multiple-range test, utilizing the SAS statistical software version 8.12 (SAS Institute, Cary, NC). Differences were considered significant at $P < 0.05$.

RESULTS

DIM Feeding Inhibits Prostate Cancer Development in TRAMP Mice

At the time of sacrifice (22 wk of age), the body weights between the normal and transgenic animals did not differ substantially. Additionally, DIM feeding did not affect body weights in either the normal or the transgenic mice (Figure 1A). Kaplan-Lefko et al. [29] reported that the GU tract—including the bladder, urethra, seminal vesicles, ampullary gland, and prostate—weight increases as a function of cancer progression in TRAMP mice. In the current study, the GU weight of TRAMP mice was increased markedly as compared to the nontransgenic (normal) mice, and this increase was suppressed significantly via the oral administration of 10 mg/kg of DIM (Figure 1B). According to the report of Kaplan-Lefko et al. [29], PIN and WDC in the DP are the predominant lesions detected in 8- and 20-week-old TRAMP mice, respectively. H&E staining of the DP demonstrated that WDC characterized by increased quantities of small glands was a predominant feature in the 22-week-old vehicle-fed TRAMP mice, whereas

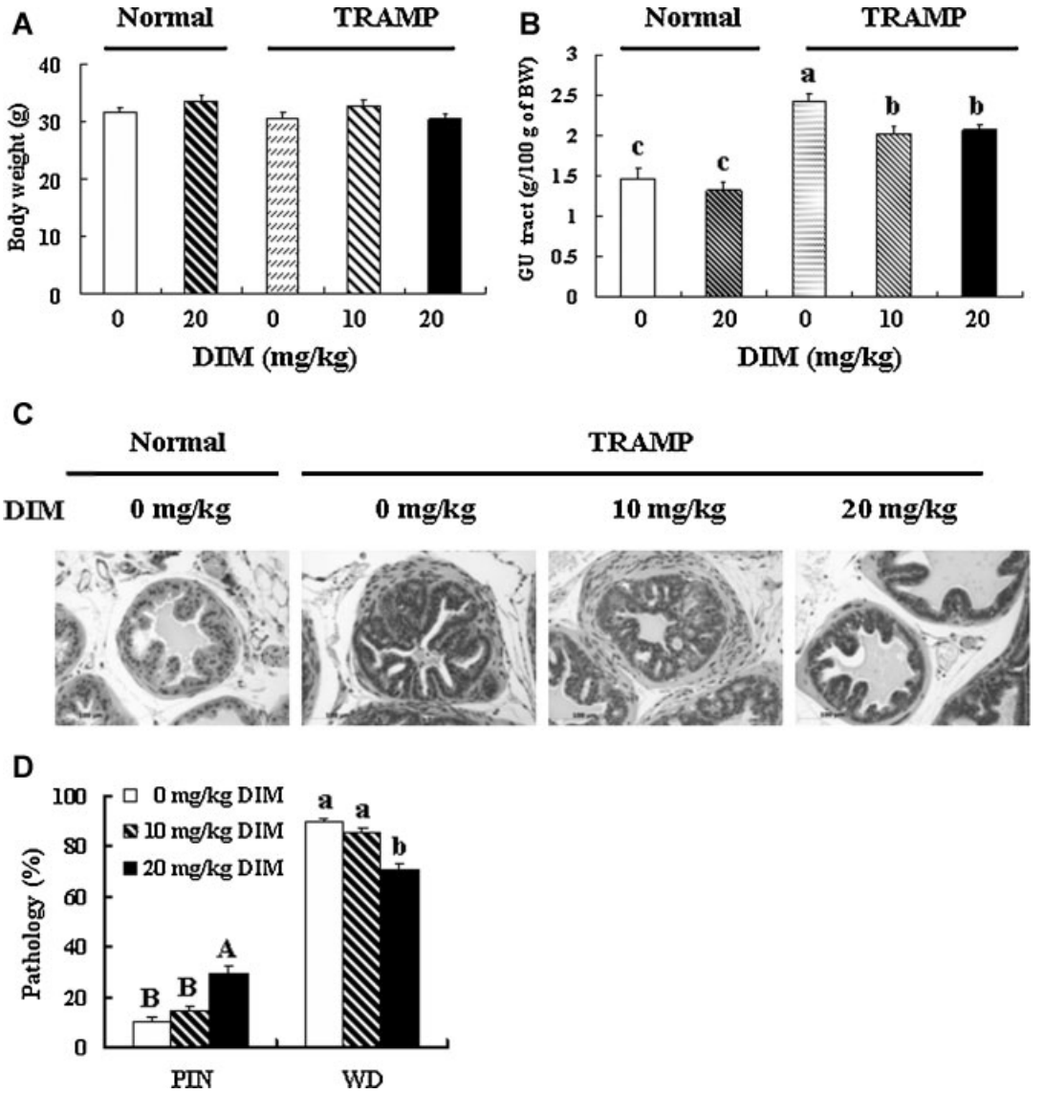

Figure 1. DIM feeding inhibits GU weight in TRAMP mice. TRAMP mice and their nontransgenic littermates were exposed to DIM via gavage as described in the Materials and Methods section. (A) The body weights of nontransgenic (0 and 20 mg/kg DIM-fed) and transgenic (0, 10, and 20 mg/kg DIM-fed) male mice at 22 wk of age are shown. (B) All mice were sacrificed at 22 wk of age, and the GU tract—including the bladder, urethra, seminal vesicles, ampullary gland, and prostate—was removed and weighed. Each bar represents the mean ± SEM ($n = 8$). (C) The prostate was fixed in 4% paraformaldehyde, and the DP was stained with H&E (×200). (D) Each bar represents the percentage (mean ± SEM) of each pathologic grade in the DP of TRAMP mice ($n = 8$). PIN, prostatic intraepithelial neoplasia; WDC, well-differentiated carcinoma. Means without the same letter differ, $P < 0.05$.

the number of lobes with WDC was reduced and the number of lobes with PIN was increased by feeding with 20 mg/kg of DIM (Figure 1C and D). These results indicate that DIM feeding delays the development of prostate cancer in TRAMP mice.

DIM Feeding Reduces Proliferation Index and Increases Apoptosis in the DP of TRAMP Mice

Immunohistochemical staining for T-ag and PCNA in the DP are shown in Figure 2. As compared to vehicle-fed TRAMP mice, the proportions of T-ag and PCNA positive cells were reduced significantly in the DP of TRAMP mice fed on 20 mg/kg of DIM. The expression of CDK2, CDK4, and cyclin A in the DP were increased in the TRAMP mice as compared with the non-TRAMP mice, and these increases were inhibited significantly by DIM feeding (20 mg/kg) (Figure 3). The expression of p27 was also increased in the TRAMP mice, and p27 expression was elevated further by DIM feeding (20 mg/kg; Figure 3). Furthermore, the number of TUNEL-positive apoptotic cells (Figure 2) and the amount of Bax expression (Figure 3) were increased, whereas the levels of Bcl-xL expression (Figure 3) were reduced in TRAMP mice fed on 20 mg/kg of DIM, as compared to the vehicle-fed TRAMP mice. However, DIM feeding did not

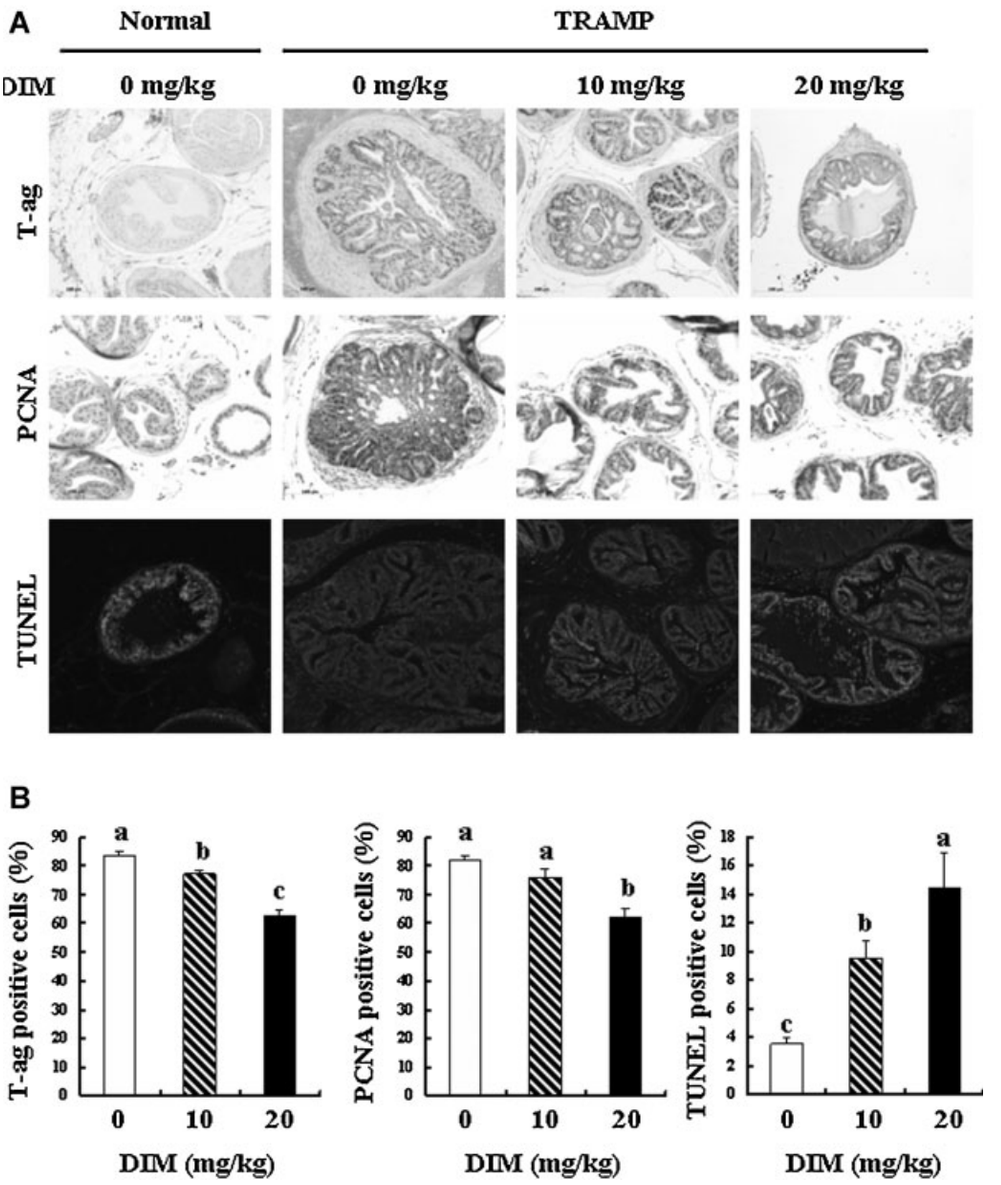

Figure 2. DIM feeding reduces PCNA expression and increases apoptosis in the DP of TRAMP mice. (A) Immunohistochemical staining for T-ag and PCNA in the DP was based on 3,3′-diaminobenzidine staining as described in the Materials and Methods section. Apoptosis was analyzed via TUNEL staining using a DeadEnd™ Fluorometric TUNEL System (Promega). Sections were counterstained with propidium iodide. (B) T-ag or PCNA positive cells were quantified by counting the number of brown-stained cells among the total cells. TUNEL-positive cells were quantified by counting green fluorescence-positive cells among the total cells. Each bar represents the mean ± SEM ($n = 5$). Means without the same letter differ, $P < 0.05$.

affect the expression of CDK2, CDK4, cyclin A, p27, Bax, or Bcl-xL in normal mice (data not shown). These data indicate that the DIM-mediated inhibition of prostate carcinogenesis was due, at least in part, to the suppression of cell cycle progression and the induction of apoptosis.

DIM Inhibits Growth and Induces Apoptosis of Prostate Cancer Cells

In order to evaluate the effects of DIM on prostate cancer development in greater detail, we conducted in vitro experiments using LNCaP and DU145 human prostate cancer cells. The results of the MTT assays showed that DIM induced dose-dependent reductions in the number of viable cells in both DU145 and LNCaP cell lines at concentrations of 10–30 μmol/L (Figure 4A). When this study was being conducted, Vivar et al. [10] reported that DIM induced a G1 arrest, inhibited the expression of CDK2 and CDK4 proteins, and increased $p27^{KIP1}$ expression in LNCaP and DU145 cells. Additionally, the DIM-induced apoptosis of prostate cancer cells

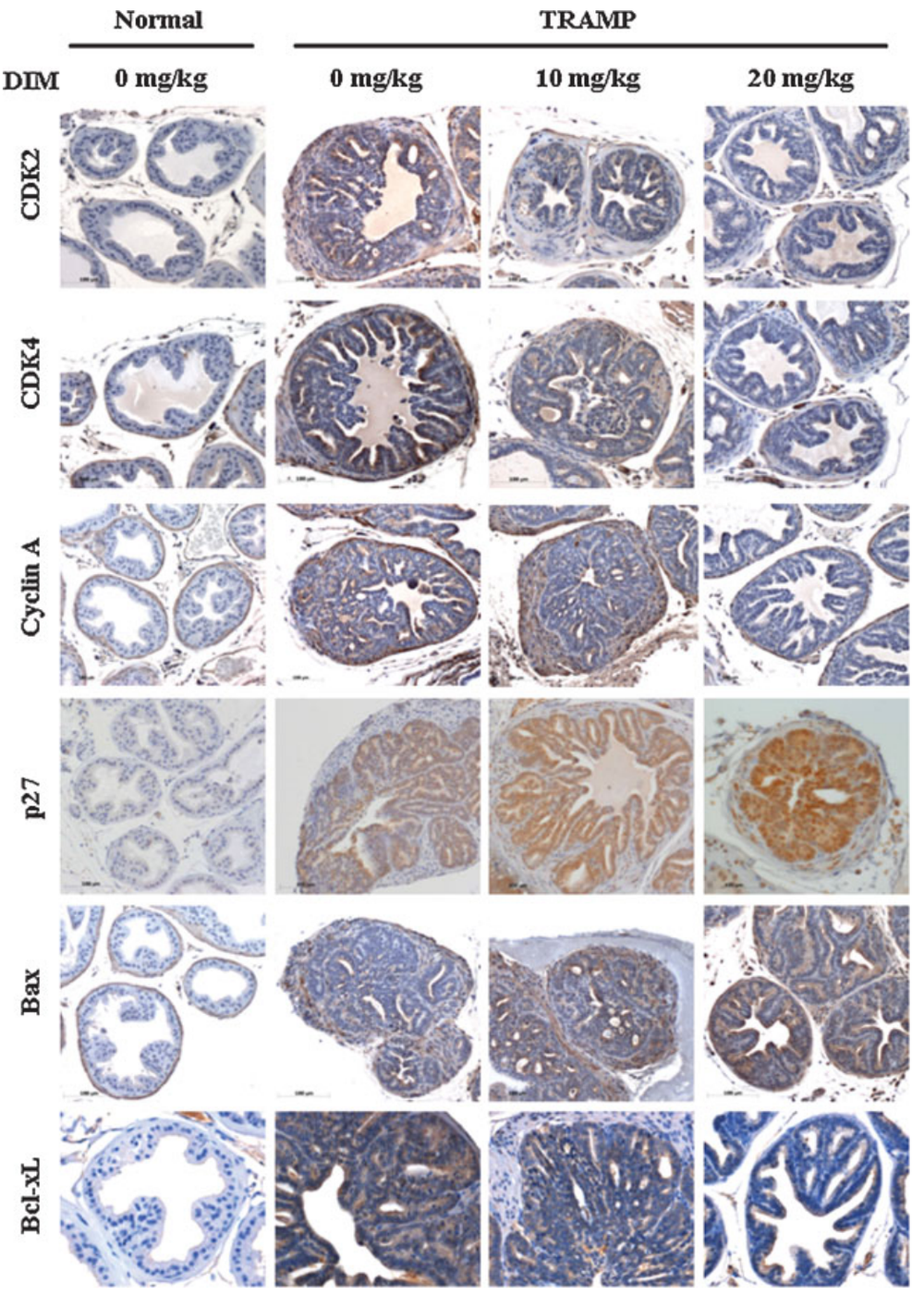

Figure 3. DIM feeding reduces CDK, cyclin A, and Bcl-xL expression and increases p27 and Bax expression in the prostate epithelium. Immunohistochemical staining for CDKs, cyclin A, p27, Bax, and Bcl-xL was based on 3,3′-diaminobenzidine staining as described in the Materials and Methods section. Sections were counterstained with hematoxylin. Photographs of immunohistochemical staining, which are representative of six different animals, are shown.

has been previously reported [11,12,30]. Therefore, in the current study we attempted to assess in detail the mechanisms by which DIM induces the apoptosis of DU145 and LNCaP cells. The translocation of phosphatidylserine from the inner leaflet of the plasma membrane to the outer leaflet was determined by staining the cells with annexin V and 7-AAD followed by flow cytometry. As is shown in

Figure 4B, the numbers of apoptotic cells were increased in DU145 cells treated with 30 μmol/L of DIM and LNCaP cells treated with 20 μmol/L of DIM for 48 h. In order to determine whether DIM induces apoptosis in a time-dependent manner, we quantitatively analyzed the mono- and oligo-nucleosomes released into the cytoplasm. Apoptosis was detected in DU145 cells at 24 h after treatment with 30 μmol/L of DIM, and had increased more profoundly at 48 h (Figure 4C).

The results of Western blot analysis of total cell lysates demonstrated that the levels of cleaved caspase-8, -9, -3, and -7 were increased in DU145 cells treated with 30 μmol/L of DIM. Pro-caspase-8

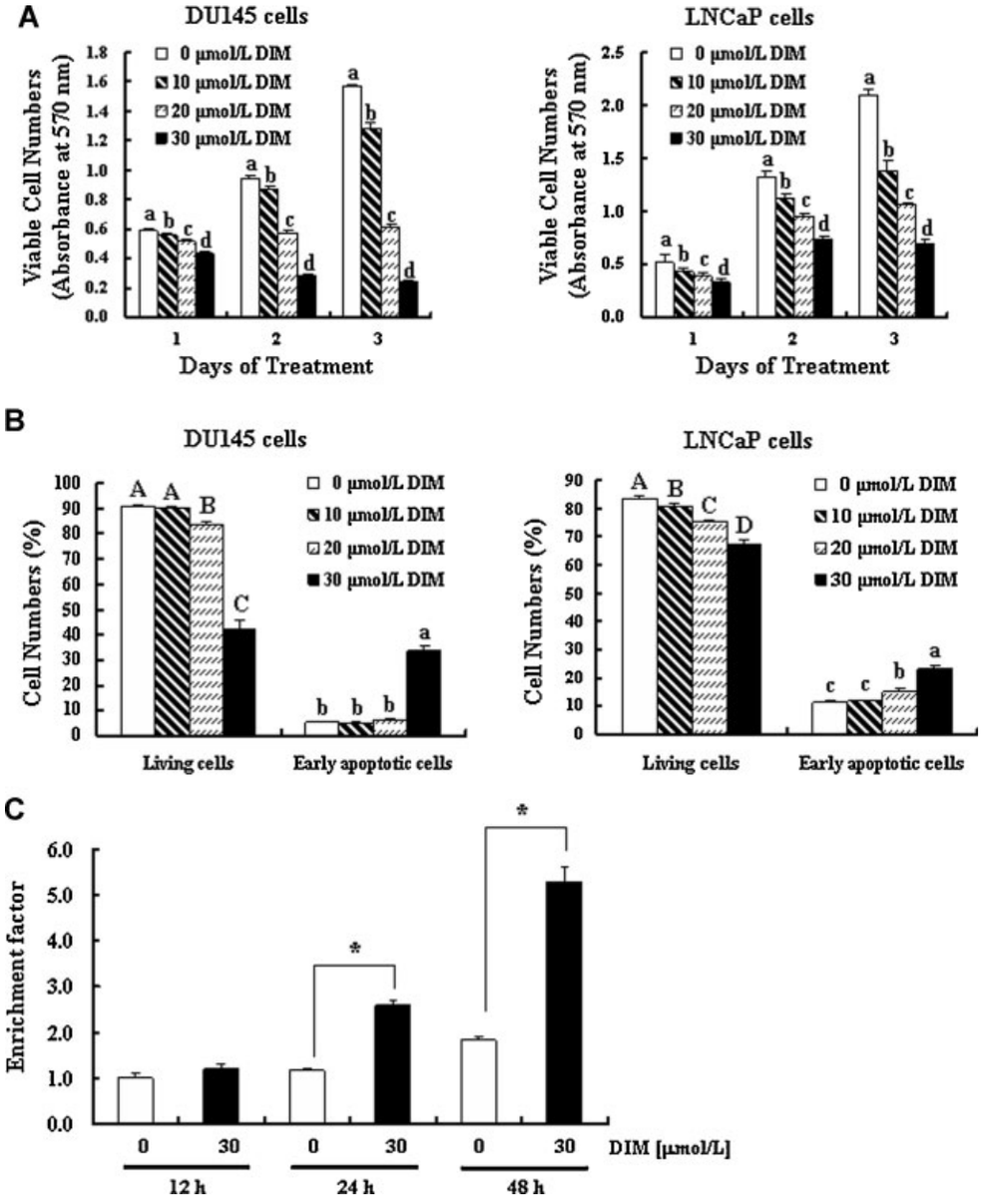

Figure 4. DIM induces apoptosis and increases the protein levels of cleaved caspases in prostate cancer cells. DU145 and LNCaP cells were plated and treated with various concentrations of DIM as described in the Materials and Methods section. (A) Viable cell numbers were estimated via an MTT assay. (B) Cells were trypsinized, stained with 7-amino-actinomycin D and annexin V, and subsequently analyzed via flow cytometry. The number of living cells and early apoptotic cells is expressed as a percentage of the total cell number. (C) Cells were treated with 0 or 30 μmol/L DIM for 12, 24, or 48 h. Apoptosis was measured using a Cell Death Detection ELISA^{PLUS} kit (Roche). Each bar represents the mean ± SEM ($n = 6$). (D) Total cell lysates were analyzed by Western blotting with their relevant antibodies. Photographs of chemiluminescent detection of the blots, which are representative of three independent experiments, are shown. The relative abundance of each band was quantified. The adjusted mean ± SEM of each band is shown above each blot. Means without a common letter differ, $P < 0.05$.

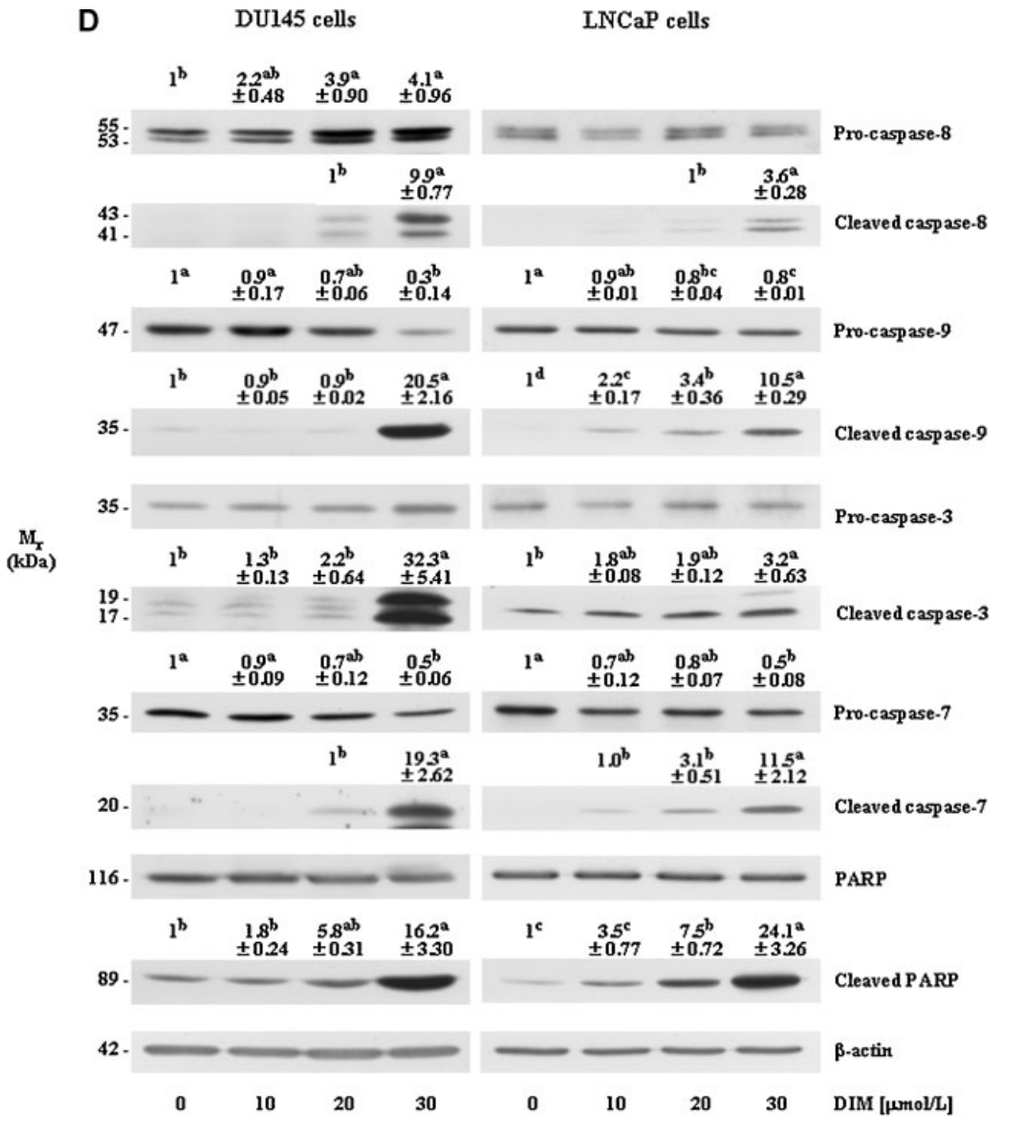

Figure 4. (*Continued*)

levels were increased and pro-caspase-3 levels remained unaltered. However, the levels of pro-caspase-9 and -7 were reduced in the DIM-treated DU145 cells. In LNCaP cells, the increases in cleaved caspase-8, -9, -3, and -7 were principally DIM dose-dependent. The levels of pro-caspase-9 and -7 were reduced, whereas the levels of pro-caspase-8 and -3 were unaltered in the DIM-treated LNCaP cells (Figure 4D). Additionally, caspase-3 activity was quantified using DEVE-*p*NA as a substrate. Caspase-3 activity was increased significantly in the cells treated with 30 μmol/L of DIM (306.3 ± 2.43% in DU145 and 177.2 ± 2.53% in LNCaP cells). The levels of cleaved PARP were also increased in both cell types treated with DIM. The levels of intact PARP were not altered by DIM treatment (Figure 4D).

DIM Increases the Release of Cytochrome c and Smac/Diablo from Mitochondria and Mitochondrial Membrane Permeability in DU145 Cells

Building on the finding that DIM induced caspase-9 activation, we further attempted to determine whether or not DIM induces the release of cytochrome c from the mitochondria. The levels of cytochrome c and Smac/Diablo were increased significantly in the cytoplasm of cells treated with 30 μmol/L DIM (Figure 5A). Because DIM was shown to induce cytochrome c release, we attempted to determine whether DIM induces mitochondrial membrane depolarization by staining cells with the mitochondrial-selective dye JC-1, followed by flow cytometry. JC-1 forms aggregates that emit a red

fluorescence in normal polarized mitochondria. Upon the depolarization of the mitochondrial membrane, JC-1 forms monomers that emit only green fluorescence [31]. The number of cells with depolarized mitochondrial membranes was shown to increase in a DIM concentration-dependent manner (Figure 5B). The increase in mitochondrial membrane permeability was detected within 12 h after the treatment of DU145 cells with 30 μmol/L of DIM and increased more profoundly at 24 h (Figure 5C).

DIM Alters the Levels of Bcl-2 Family Proteins in DU145 Cells

As the permeability of mitochondrial membranes was increased in DIM-treated cells, we next evaluated the effects of DIM on the levels of Bcl-2 family proteins via Western blotting. As is shown in Figure 5D, DIM induced a significant increase in the levels of Bax and truncated Bid (t-Bid) at 48 h. The levels of Bcl-xL were reduced in cells treated with 30 μmol/L of DIM, whereas the levels of Bcl-2 were not altered by DIM treatment. An increase in Bax expression and a reduction in Bcl-xL expression were detected within 12 h after DIM treatment (Figure 5E).

A Caspase-8 Inhibitor Mitigates DIM-Induced Apoptosis in DU145 Cells

Because DIM increased the levels of cleaved caspase-8 (Figure 4D) and t-Bid (Figure 5D), the effects of DIM on Fas and membrane-bound Fas ligand (Fas-L) were assessed using Western blotting. DIM increased the levels of Fas and Fas-L in DU145 cells (Figure 6A). As DIM increased caspase-8 activation and Bid cleavage, we subsequently attempted to determine whether the pretreatment of cells with Z-IETD-FMK (a caspase-8 inhibitor) could inhibit DIM-induced apoptotic cell death. The treatment of DU145 cells with 30 μmol/L of DIM significantly reduced the number of living cells and increased the number of apoptotic cells. The caspase-8 inhibitor induced a decline in DIM-induced apoptosis (Figure 6B). Additionally, treatment with a caspase-8 inhibitor significantly reduced DIM-induced increases in the levels of cleaved caspase-3, t-Bid, and cleaved PARP (Figure 6C).

DISCUSSION

I3C is naturally present in cruciferous vegetables such as cabbage, broccoli, Brussels sprouts, and kale, and was shown recently to inhibit the tumor growth of subcutaneously injected TRAMP-C2 xenografts [32]. I3C is an unstable compound and, upon ingestion, is converted into several condensation products, among which DIM is the principal product [9]. DIM has been demonstrated to inhibit cell cycle progression and induce apoptosis in prostate cancer cells in culture [10–12]. Additionally, DIM has been shown to inhibit the growth of TRAMP-C2 cells injected subcutaneously into C57BL/6 mice [15]. Because the TRAMP mouse model is closely reflective of the histological progression of human prostate cancer, the present study attempted to determine whether DIM feeding inhibits prostate cancer development in TRAMP mice. We demonstrated that DIM feeding suppresses the increase in GU weights and T-ag expression and delays the histological progression of prostate cancer. We also demonstrated that DIM feeding suppresses the expression of PCNA and induces apoptosis in the DP of TRAMP mice. Furthermore, the anti-proliferative and pro-apoptotic effects of DIM on TRAMP mice are associated with the alteration of cell cycle modulators (CDK2, CDK4, cyclin A, and p27) and Bcl-2 family proteins (Bax and Bcl-xL), respectively (Figure 7). These results are consistent with the in vitro results obtained in the present study (Figure 5) and by Vivar et al. [10]. Together, these results indicate that DIM may have some potential for use as a chemopreventive agent for prostate cancer.

Kaplan-Lefko et al. [29] have demonstrated that androgen receptor (AR) was expressed during cancer progression, but its levels were reduced or absent in late-stage TRAMP mice. In both AR-positive LNCaP and AR-negative DU145 cells, we noted that DIM decreased cell viability (Figure 4A). We also noted that DIM inhibited the expression of PCNA (Figure 2), cyclin A, CDK2, and CDK4 and increased p27 expression (Figure 3) in the DP in TRAMP mice, as shown by immunohistochemical staining. Furthermore, a recent report showed that DIM induced a G1 arrest in LNCaP and DU145 cells via the inhibition of CDK2 and CDK4 expression and the induction of p27 expression [10]. Collectively, these results show that DIM inhibits the cell cycle progression of prostate cancer cells via the inhibition of CDK activity.

The number of TUNEL-positive apoptotic cells (Figure 2) and Bax expression levels (Figure 3) were increased, whereas Bcl-xL (Figure 3) expression was decreased in the DP of DIM-fed TRAMP mice as compared to the mice fed with vehicle only. Our in vitro data obtained using DU145 cells indicated that DIM alters the levels of Bcl-2 family proteins (Bax, t-Bid, and Bcl-xL) (Figure 5D). By way of contrast, Nachshon-Kedmi et al. [12] reported that Bax expression levels were not altered in LNCaP, DU145, and PC3 cells as the result of 24 h of exposure to 75 μmol/L of DIM. Similar to our results, it was reported that Bax protein levels were increased after 48 h following treatment with 50 μmol/L DIM in human breast cancer cells [33]. Bax undergoes a conformational change in response to a death signal which results in its homodimerization and mitochondrial integral membrane insertion, and Bcl-2 or Bcl-xL can inhibit Bax activation [34]. Although future studies will be required to resolve this

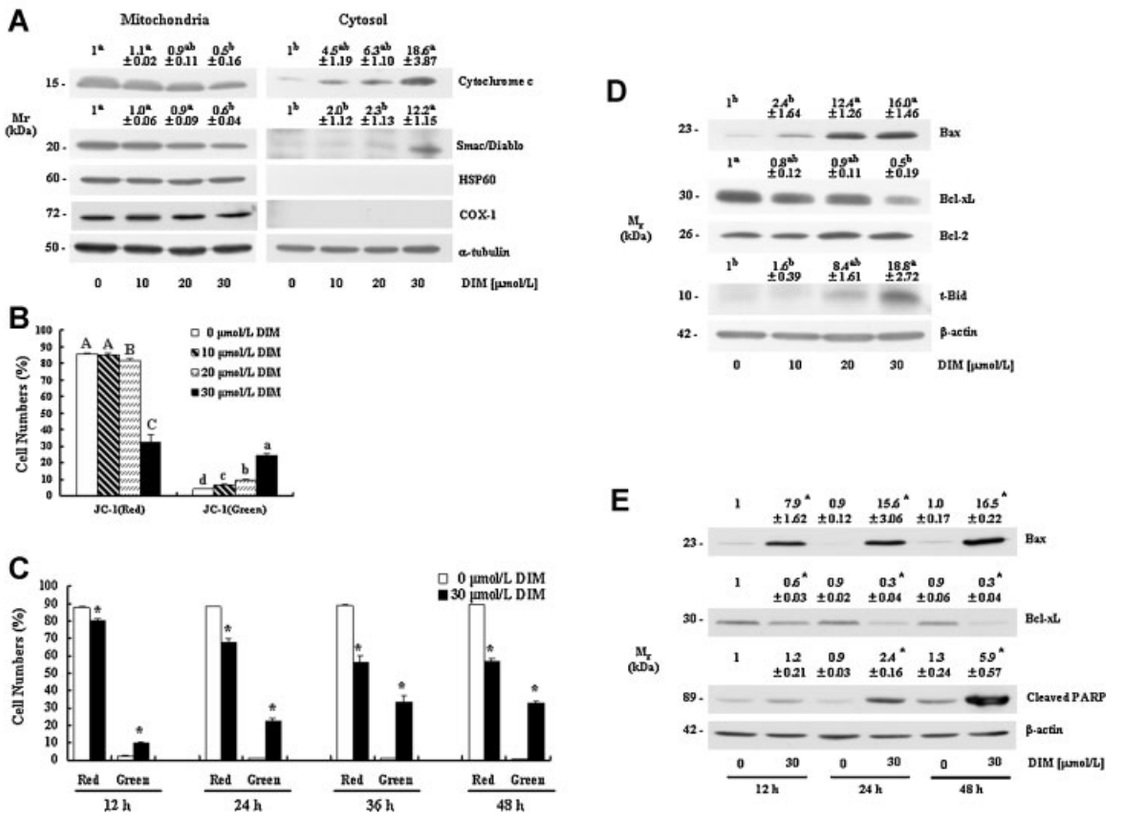

Figure 5. DIM induces mitochondrial membrane depolarization in DU145 cells. (A, B, and D) Cells were treated for 2 d with different concentrations of DIM. (C and E) Cells were treated with 30 μmol/L of DIM for 12, 24, 36, or 48 h. The cytosolic and mitochondrial fractions (A) and total cell lysates (D and E) were analyzed via Western blotting with their relevant antibodies. Photographs of chemiluminescent detection of the blots, which are representative of three independent experiments, are shown. The relative abundance of each band was quantified. The adjusted mean ± SEM of each band is shown above each blot. (B and C) Cells were loaded with JC-1 and then analyzed by flow cytometry. The number of cells with normal polarized mitochondrial membranes (red) and cells with depolarized mitochondrial membranes (green) are expressed as percentages of the total cell number. Each bar represents the mean ± SEM ($n = 6$). (A–D) Means without a common letter differ, $P < 0.05$. (E) *Different from 0 μmol/L DIM at a time, $P < 0.05$.

discrepancy, the results of the present study indicate that the alteration of Bcl-2 family proteins may have induced the permeabilization of mitochondrial membranes (Figure 5B), thereby resulting in the release of cytochrome c and Smac/Diablo from the mitochondria (Figure 5A). These events may have further triggered the activation of caspases and PARP cleavage (Figure 4D), resulting in the induction of apoptosis (Figure 4B) in DIM-treated DU145 cells. Our empirical observations revealed that DIM treatment sequentially induced the expression of Bcl-2 family proteins at 12 h (Figure 5E), the permeabilization of mitochondrial membranes at 12–24 h (Figure 5C), and PARP cleavage (Figure 5E) and apoptotic cell death at 24–48 h (Figure 4C) in DU145 cells.

The apoptotic cascade can be initiated via the activation of plasma membrane death receptors in response to ligand binding [13]. We noted that the treatment of DU145 cells with DIM resulted in dramatically increased expressions of Fas and slightly increased the levels of Fas-L (Figure 6). Although it has been previously demonstrated that Fas promotes tumor growth and also performs a variety of nonapoptotic functions depending on the experimental conditions and the involved tissues [35,36], the activation of Fas by its physiological ligand has been reported in several studies to trigger apoptosis [37,38]. Consistent with increases in Fas and Fas-L, the levels of cleaved caspase-8 were shown to have increased in DIM-treated cells, and the caspase-8 inhibitor significantly reduced DIM-mediated apoptosis and caspase-3, PARP, and Bid cleavage. These results indicate that, in addition to the mitochondrial pathway, the death receptor-dependent pathway (caspase-8 activation) is also a contributing factor in DIM-induced apoptosis. In pancreatic cancer cells, DIM has been reported to induce apoptosis via endoplasmic reticulum stress-dependent upregulations of DR5 [39]. In the current study, the effects of DIM on other death receptors such as tumor necrosis factor receptor, DR4, and DR5 were not addressed. Future studies will be required to determine whether the activation of other death

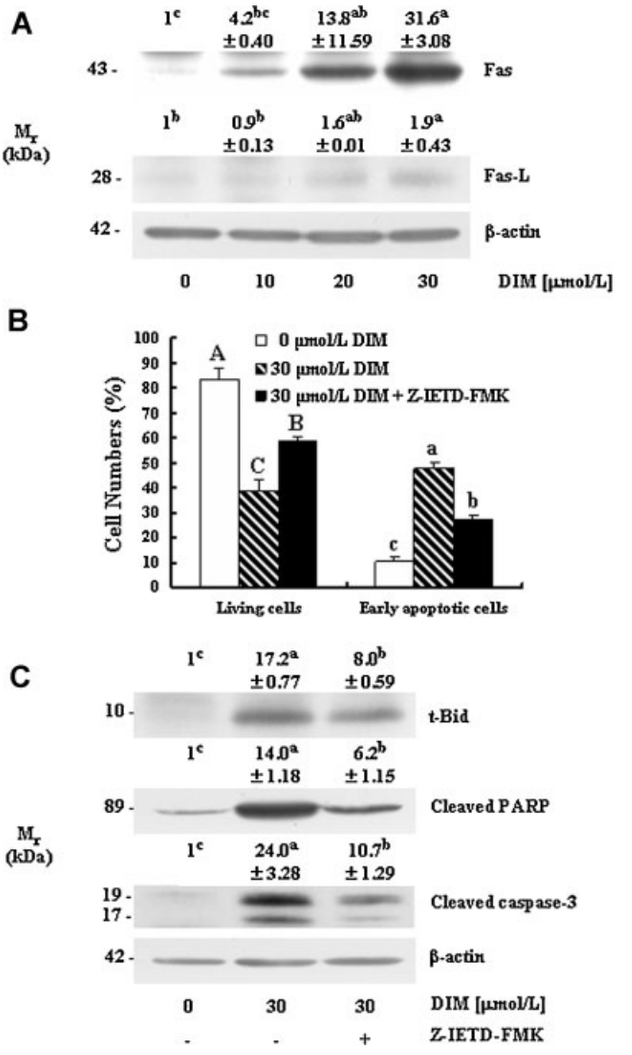

Figure 6. The caspase-8 inhibitor Z-IETD-FMK mitigates DIM-induced apoptosis in DU145 cells. (A) Cells were treated for 2 d with DIM. Total cell lysates were analyzed via Western blotting with their indicated antibodies. (B and C) Serum-deprived DU145 cells were pretreated for 4 h with 20 μmol/L Z-IETD-FMK prior to 2 d of treatment with 30 μmol/L of DIM. (B) The cells were trypsinized, stained with 7-amino-actinomycin D and annexin V-PE, and then analyzed by flow cytometry. The number of living cells and early apoptotic cells are expressed as percentages of the total cell numbers. Each bar represents the mean ± SEM ($n = 6$). (C) Total cell lysates were analyzed by Western blotting with their relevant antibodies. Photograph of chemiluminescent detection of the blots, which were representative of three independent experiments, are shown. The relative abundance of each band was quantified. The adjusted mean ± SEM of each band is shown above each blot. Means without a common letter differ, $P < 0.05$.

receptors contributes to apoptosis in DIM-treated prostate cancer cells.

In addition to the observed inhibition of cell cycle progression and the induction of apoptosis DIM may exert chemopreventive effects in the prostate via different mechanisms. As inflammatory cells and molecules can influence many aspects of cancer development and progression [40], an inflammatory microenvironment was recently suggested to be added to the list of cancer hallmarks [41]. We reported previously that DIM inhibits the inflammatory responses of murine macrophages to lipopolysaccharide stimulation [42] and attenuates dextran sodium sulfate-induced colonic inflammation and tumorigenesis in mice [43]. Whether or not DIM feeding inhibits inflammatory mediators in TRAMP mice, however, remains to be determined.

In our in vitro studies, we demonstrated that DIM induces apoptosis in human prostate cancer cells at 20–30 μmol/L. To the best of our knowledge, the distribution of DIM in the prostates of mice after oral administration of this compound has yet to be elucidated. Anderton et al. [44] reported that DIM was detected in the plasma and tissues (liver, heart, lung, kidney, and brain) after the oral administration of DIM to mice. The plasma concentrations of DIM were 19 μg/mL (0–24 h) after the oral administration of 250 mg/kg of DIM to mice. Moreover, the net

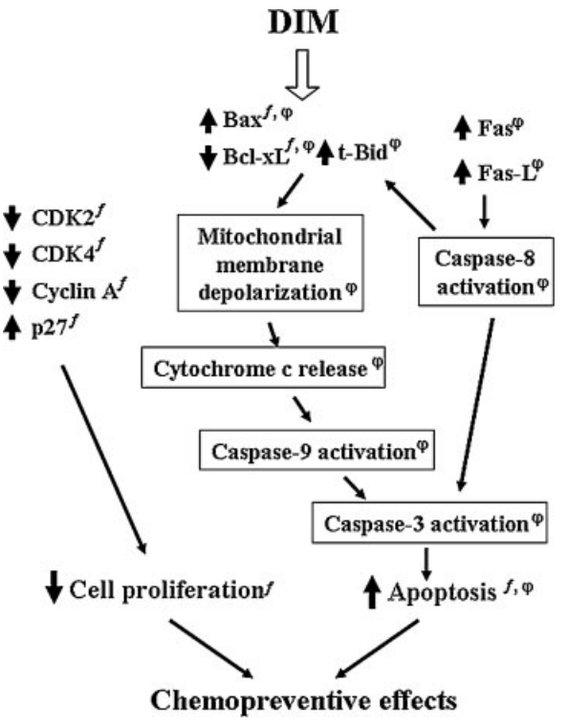

Figure 7. Proposed schemata of the mechanisms by which DIM inhibits prostate cancer development. *f* and *φ* indicate that the results were obtained from in vivo and in vitro studies, respectively.

exposure of tissues such as the liver, kidney, lung, and heart was approximately 54–129 μg/g, thus suggesting that orally administered DIM is absorbed quite well into the blood and distributed throughout the tissues. Collectively, these results are suggestive of the possibility of DIM distribution in the prostate. In the present study, we fed mice with 10–20 mg/kg of DIM. Although future studies will be required to determine what quantity of DIM reaches the plasma and the target tissues in our DIM-treated mice, one might speculate that the concentration of DIM might have reached a level of approximately 1.5 μg/mL (6 μmol/L) in the blood, and the actual concentrations of DIM in the tissues in mice fed on 20 mg/kg of DIM might have reached levels as high as 18–42 μmol/L, comparable to those used in our cell culture studies.

I3C is derived from the hydrolysis of glucobrassicin, and the concentration of glucobrassicin varies among different cruciferous vegetables and conditions, including different growing seasons [45] and technological processes [46]. As the content of I3C in vegetables of genus Brassica ranges between approximately 15–500 mg/kg of fresh weight and approximately 10–20% of the breakdown products of I3C are converted into DIM, it can be calculated that 1.5–100 mg of DIM can be formed from a single kilogram of genus Brassica. Thus, it appears that it would be difficult for humans to achieve the in vitro concentrations and in vivo doses of DIM used in the present studies simply by consuming cruciferous vegetables.

In conclusion, the results of this study demonstrated that DIM feeding delays the histological progression of prostate cancer. We also demonstrated that DIM feeding suppresses the expression of PCNA and induces apoptosis in the DP of TRAMP mice. Additionally, we have shown that DIM induces apoptosis in human prostate cancer cells (see the proposed schemata of the mechanism in Figure 7). Because TRAMP is one such model for prostate cancer that closely mimics progressive forms of human disease, the results of this study suggest that DIM might potentially prove useful as a chemopreventive agent for prostate cancer.

ACKNOWLEDGMENTS

This study was supported by the Basic Science Research Program (grant number 2008-314-F00069) and the SRC program (Center for Food & Nutritional Genomics: grant number 2010-0001886) of the National Research Foundation (NRF) of Korea, funded by the Ministry of Education, Science, and Technology.

REFERENCES

1. Jemal A, Siegel R, Ward E, et al. Cancer statistics, 2008. CA Cancer J Clin 2008;58:71–96.
2. Jones RA, Underwood SM, Rivers BM. Reducing prostate cancer morbidity and mortality in African American men: Issues and challenges. Clin J Oncol Nurs 2007;11:865–872.
3. Chan JM, Stampfer MJ, Giovannucci E, et al. Plasma insulin-like growth factor-I and prostate cancer risk: A prospective study. Science 1998;279:563–566.
4. Jain MG, Hislop GT, Howe GR, Ghadirian P. Plant foods, antioxidants, and prostate cancer risk: Findings from case-control studies in Canada. Nutr Cancer 1999;34:173–184.
5. Cohen JH, Kristal AR, Stanford JL. Fruit and vegetable intakes and prostate cancer risk. J Natl Cancer Inst 2000;92:61–68.
6. Kolonel LN, Hankin JH, Whittemore AS, et al. Vegetables, fruits, legumes and prostate cancer: A multiethnic case-control study. Cancer Epidemiol Biomarker Prev 2000;9:795–804.
7. Bradfield CA, Bjeldanes LF. High-performance liquid chromatographic analysis of anticarcinogenic indoles in Brassica oleracea. J Agric Food Chem 1987;35:46–49.
8. Sarkar FH, Li Y. Indole-3-carbinol and prostate cancer. J Nutr 2004;134:3493S–3498S.
9. De Kruif CA, Marsman JW, Venekamp JC, et al. Structure elucidation of acid reaction products of indole-3-carbinol: Detection in vivo and enzyme induction in vitro. Chem Biol Interact 1991;80:303–315.
10. Vivar OI, Lin CL, Firestone GL, Bjeldanes LF. 3,3′-Diindolylmethane induces a G(1) arrest in human prostate cancer cells irrespective of androgen receptor and p53 status. Biochem Pharmacol 2009;78:469–476.
11. Nachshon-Kedmi M, Yannai S, Fares FA. Induction of apoptosis in human prostate cancer cell line, PC3, by 3,3′-diindolylmethane through the mitochondrial pathway. Br J Cancer 2004;91:1358–1363.
12. Nachshon-Kedmi M, Yannai S, Haj A, Fares FA. Indole-3-carbinol and 3,3′-diindolylmethane induce apoptosis in human prostate cancer cells. Food Chem Toxicol 2003;41:745–752.

13. Ashkenazi A, Dixit VM. Death receptors: Signaling and modulation. Science 1998;281:1305–1308.
14. Vander Heiden MG, Thompson CB. Bcl-2 proteins: Regulators of apoptosis or of mitochondrial homeostasis? Nat Cell Biol 1999;1:E209–E216.
15. Nachshon-Kedmi M, Fares FA, Yannai S. Therapeutic activity of 3,3′-diindolylmethane on prostate cancer in an in vivo model. Prostate 2004;61:153–160.
16. Killion JJ, Radinsky R, Fidler IJ. Orthotopic models are necessary to predict therapy of transplantable tumors in mice. Cancer Metastasis Rev 1998;17:279–284.
17. Greenberg NM, DeMayo F, Finegold MJ, et al. Prostate cancer in a transgenic mouse. Proc Natl Acad Sci USA 1995;92:3439–3443.
18. Gingrich JR, Barrios RJ, Morton RA, et al. Metastatic prostate cancer in a transgenic mouse. Cancer Res 1996;56:4096–4102.
19. Rokhlin OW, Bishop GA, Hostager BS, et al. Fas-mediated apoptosis in human prostatic carcinoma cell lines. Cancer Res 1997;57:1758–1768.
20. Bookstein R, Shew JY, Chen PL, Scully P, Lee WH. Suppression of tumorigenicity of human prostate carcinoma cells by replacing a mutated RB gene. Science 1990;247:712–715.
21. Rokhlin OW, Gudkov AV, Kwek S, Glover RA, Gewies AS, Cohen MB. p53 is involved in tumor necrosis factor-alpha-induced apoptosis in the human prostatic carcinoma cell line LNCaP. Oncogene 2000;19:1959–1968.
22. Greenberg NM, DeMayo FJ, Sheppard PC, et al. The rat probasin gene promoter directs hormonally and developmentally regulated expression of a heterologous gene specifically to the prostate in transgenic mice. Mol Endocrinol 1994;8:230–239.
23. Gingrich JR, Barrios RJ, Foster BA, Greenberg NM. Pathologic progression of autochthonous prostate cancer in the TRAMP model. Prostate Cancer Prostatic Dis 1999;2:70–75.
24. Jung JI, Lim SS, Choi HJ, et al. Isoliquiritigenin induces apoptosis by depolarizing mitochondrial membranes in prostate cancer cells. J Nutr Biochem 2006;17:689–696.
25. Cho HJ, Kim WK, Kim EJ, et al. Conjugated linoleic acid inhibits cell proliferation and ErbB3 signaling in HT-29 human colon cell line. Am J Physiol 2003;284:G996–G1005.
26. Eguchi Y, Srinivasan A, Tomaselli KJ, Shimizu S, Tsujimoto Y. ATP-dependent steps in apoptotic signal transduction. Cancer Res 1999;59:2174–2181.
27. Koll H, Guiard B, Rassow J, et al. Antifolding activity of hsp60 couples protein import into the mitochondrial matrix with export to the intermembrane space. Cell 1992;68:1163–1175.
28. Tokuyama Y, Reddy AP, Bethea CL. Neuroprotective actions of ovarian hormones without insult in the raphe region of rhesus macaques. Neuroscience 2008;154:720–731.
29. Kaplan-Lefko PJ, Chen TM, Ittmann MM, et al. Pathobiology of autochthonous prostate cancer in a pre-clinical transgenic mouse model. Prostate 2003;55:219–237.
30. Rahman KM, Banerjee S, Ali S, et al. 3,3′-Diindolylmethane enhances taxotere-induced apoptosis in hormone-refractory prostate cancer cells through survivin down-regulation. Cancer Res 2009;69:4468–4475.
31. Smiley ST, Reers M, Mottola-Hartshorn C, et al. Intracellular heterogeneity in mitochondrial membrane potentials revealed by a J-aggregate-forming lipophilic cation JC-1. Proc Natl Acad Sci USA 1991;88:3671–3675.
32. Souli E, Machluf M, Morgenstern A, Sabo E, Yannai S. Indole-3-carbinol (I3C) exhibits inhibitory and preventive effects on prostate tumors in mice. Food Chem Toxicol 2008;46:863–870.
33. Hong C, Firestone GL, Bjeldanes LF. Bcl-2 family-mediated apoptotic effects of 3,3′-diindolylmethane (DIM) in human breast cancer cells. Biochem Pharmacol 2002;63:1085–1097.
34. Gross A, Jockel J, Wei MC, Korsmeyer SJ. Enforced dimerization of BAX results in its translocation, mitochondrial dysfunction and apoptosis. EMBO J 1998;17:3878–3885.
35. Chen L, Park SM, Tumanov AV, et al. CD95 promotes tumour growth. Nature 465:492–496.
36. Peter ME, Budd RC, Desbarats J, et al. The CD95 receptor: Apoptosis revisited. Cell 2007;129:447–450.
37. Krammer PH. CD95's deadly mission in the immune system. Nature 2000;407:789–795.
38. Nagata S. Apoptosis by death factor. Cell 1997;88:355–365.
39. Abdelrahim M, Newman K, Vanderlaag K, Samudio I, Safe S. 3,3′-Diindolylmethane (DIM) and its derivatives induce apoptosis in pancreatic cancer cells through endoplasmic reticulum stress-dependent upregulation of DR5. Carcinogenesis 2006;27:717–728.
40. Mantovani A, Allavena P, Sica A, Balkwill F. Cancer-related inflammation. Nature 2008;454:436–444.
41. Mantovani A. Cancer: Inflaming metastasis. Nature 2009;457:36–37.
42. Cho HJ, Seon MR, Lee YM, et al. 3,3′-Diindolylmethane suppresses the inflammatory response to lipopolysaccharide in murine macrophages. J Nutr 2008;138:17–23.
43. Kim YH, Kwon HS, Kim DH, et al. 3,3′-Diindolylmethane attenuates colonic inflammation and tumorigenesis in mice. Inflamm Bowel Dis 2009;15:1164–1173.
44. Anderton MJ, Manson MM, Verschoyle R, et al. Physiological modeling of formulated and crystalline 3,3′-diindolylmethane pharmacokinetics following oral administration in mice. Drug Metab Dispos 2004;32:632–638.
45. Cartea ME, Velasco P, Obregon S, Padilla G, de Haro A. Seasonal variation in glucosinolate content in Brassica oleracea crops grown in northwestern Spain. Phytochemistry 2008;69:403–410.
46. Cieslik E, Leszczynska T, Filipiak-Florkiewicz A, Sikora E, Pisulewski PM. Effects of some technological processes on glucosinolate contents in cruciferous vegetables. Food Chem 2007;105:976–981.